JACS
JOURNAL OF THE AMERICAN CHEMICAL SOCIETY
Article
pubs.acs.org/JACS

A Proton-Switchable Bifunctional Ruthenium Complex That Catalyzes Nitrile Hydroboration

Jacob B. Geri and Nathaniel K. Szymczak*

Department of Chemistry, University of Michigan, 930 N. University, Ann Arbor, Michigan 48109-1055, United States

Supporting Information

ABSTRACT: A new bifunctional pincer ligand framework bearing pendent proton-responsive hydroxyl groups was prepared and metalated with Ru(II) and subsequently isolated in four discrete protonation states. Stoichiometric reactions with H_2 and HBPin showed facile E−H (E = H or BPin) activation across a Ru(II)−O bond, providing access to unusual Ru−H species with strong interactions with neighboring proton and boron atoms. These complexes were found to promote the catalytic hydroboration of ketones and nitriles under mild conditions, and the activity was highly dependent on the ligand's protonation state. Mechanistic experiments revealed a crucial role of the pendent hydroxyl groups for catalytic activity.

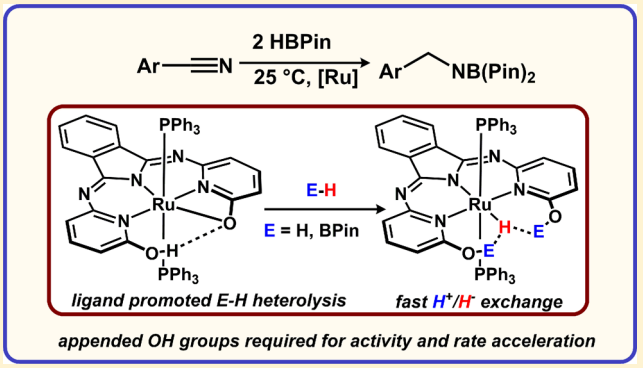

INTRODUCTION

Proton-switchable catalysis is widely used in biological systems as a means to gate reactivity and facilitate otherwise incompatible reaction sequences.[1] Modification of a given proton gradient can be used to induce reversible geometric changes[2] and modulate electronic density at a metal site,[3] and collectively, these can be used as a switch for catalytic activity. To mimic such function, metal complexes containing proton responsive ligands have recently been shown to exhibit pH dependent activity that enables on/off switching.[4] Such bifunctional metal complexes have emerged as efficient catalysts for (transfer) hydrogenation[5] and hydrofunctionalization[6] reactions. These transformations rely on the cooperative activation of E−H bonds (E = H, BR_2, or SiR_3) and subsequent transfer of reactive electrophilic and nucleophilic moieties to polar substrates.

Metal−ligand constructs with multiple accessible protonation states can impart a high level of control over reaction initiation as well as activity.[7] However, the regulation of activity among three or more discrete protonation states is underdeveloped. While there are several examples of catalytic systems that respond to protonation/deprotonation, they are usually limited to two isolable species, and characterization of multiple (>2) protonation states is rare.[4,8] In addition to a "base activation" strategy whereby a single proton transfer event turns on catalysis, further modulation of a catalyst's protonation state can also dramatically tune nucleophilicity at a metal site[3a,9] and allow further control over catalytic activity. Our group is working to evaluate how the precise structural, electronic, and cooperative modes of a metal's secondary coordination sphere can be used to regulate reactivity and has developed ligands with appended polar groups to assess their ability to influence subsequent reactivity.[10]

In contrast to the intense attention paid to the development of proton-responsive hydrogenation catalysts, cooperative activation of weakly nucleophilic B−H bonds to effect polar bond reduction remains relatively unexplored.[6b,c,11,12] Despite significant advances in the reduction of nitriles over the last three decades, there remain challenging selectivity problems.[13] For instance, harsh reductants such as main group hydrides show poor selectivity for nitriles in the presence of carbonyl-containing functional groups,[14,15] while heterogeneous hydrogenation of nitriles is incompatible with functional groups susceptible to hydrogenolysis.[16] Due to the problems associated with reagent compatibility, investigations into catalysts that promote nitrile hydroboration are under active investigation,[11b,17] and bifunctional complexes are uniquely situated for this purpose (Figure 1).

We recently reported a series of ruthenium complexes containing an *N,N,N*-bMepi pincer ligand (bMepi = 1,3-bis(6′-methyl-2′-pyridylimino)isoindolate), which are highly active

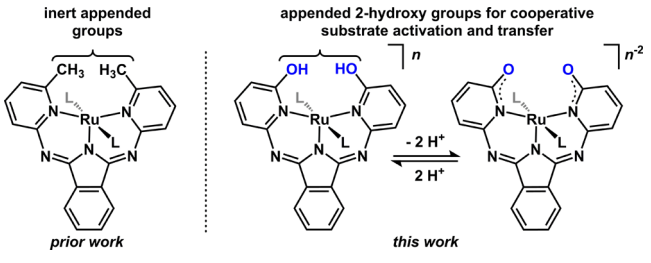

Figure 1. Conceptual development of bis(2′-hydroxy-6′-imino-pyridyl)isoindolene (BH3PI).

Received: January 18, 2015
Published: October 1, 2015

DOI: 10.1021/jacs.5b08406
J. Am. Chem. Soc. 2015, 137, 12808−12814

precatalysts for the dehydrogenation of alcohols and amines.[18] We hypothesized that by modifying the *ortho* substituents from inert $-CH_3$ to reactive $-OH$ groups, we could bias the system for bifunctional E−H activation pathways and also provide access to protonation state dependent catalysis (Figure 1).[7,19] In this Article, we report the development of a new ligand platform, bis(2′-hydroxy-6′-iminopyridyl)isoindoline (BH_3PI; H_x denotes the available proton inventory of the ligand framework), and its associated ruthenium complexes in four protonation states and showcase the ability of these complexes to promote extremely rapid, proton-switchable, and responsive catalysis for ketone and nitrile hydroboration.

RESULTS AND DISCUSSION

Synthesis, Characterization, and Structural Features of Designed Complexes. We prepared BH_3PI by a three-step synthetic protocol from commercially available reagents (Figure 2). Condensation of 2-bromo-6-aminopyridine and phthalonitrile afforded bis(2′-bromo-6′-iminopyridyl)isoindoline in 73% yield. Nucleophilic substitution with sodium benzyl oxide proceeded in 71% yield, and the resulting benzyl ether was deprotected in neat BBr_3 to provide the ligand (BH_3PI) in 74% yield as a red powder; the preparation can be scaled to gram quantities.

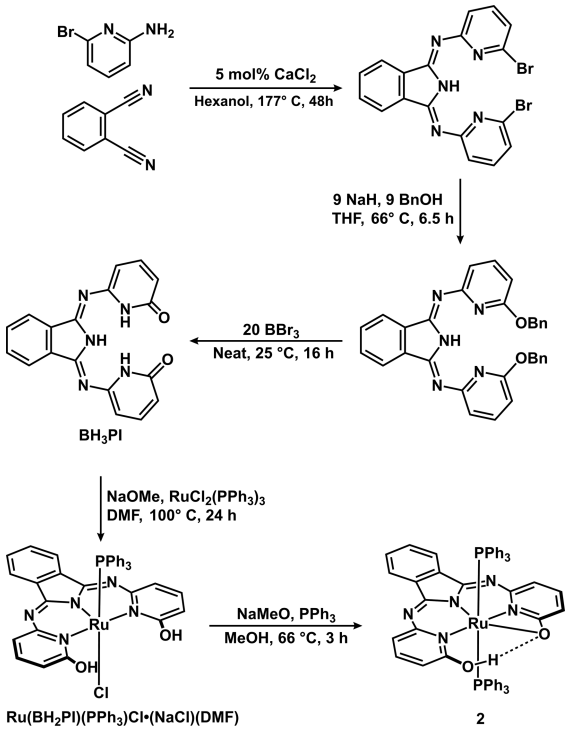

Figure 2. Synthesis of BH3PI and **2**.

We assessed whether a metal−BH_3PI complex was able to accommodate multiple protonation states (of use for the cooperative activation of small molecules) by examining its ruthenium(II) complexes. $Ru(BH_2PI)(PPh_3)Cl\cdot(NaCl)(DMF)$ was prepared by treating $Ru(PPh_3)_3Cl_2$ with BH_3PI in the presence of 1 equiv of $NaOCH_3$ in DMF solvent. Following dehydrohalogenation with another equiv of $NaOCH_3$ in the presence of PPh_3, $RuBH_1PI(PPh_3)_2$ (**2**) was obtained in 54% yield (Figure 2). NMR spectroscopic analysis revealed a C_2-symmetric set of ligand resonances, consistent with fast exchange of the single acidic proton, and the ^{31}P NMR spectrum revealed a singlet at δ 33.6, consistent with *trans*-disposed PPh_3 ligands. This complex was a useful synthon for further proton transfer reactivity. For instance, addition of 1 equiv of trifluoroacetic acid (CF_3COOH) afforded $RuBH_2PI(PPh_3)_2(CF_3CO_2)$ (**3**, Figure 3) in quantitative yield, as noted by the appearance of a new resonance at δ 32.0 in the ^{31}P NMR spectrum. Further protonation of **3** using 2 equiv of CF_3COOH afforded **4**. NMR spectroscopy revealed that protons in the complex were in rapid exchange, reflected in the observation of one acidic proton resonance at δ 13.84 at room temperature. Alternatively, the addition of 1 equiv of potassium bis(trimethylsilyl)amide ($KN(Me_3Si)_2$) to **2** in the presence of 18-crown-6 afforded the deprotonated complex, $[Ru(BH_0PI)(PPh_3)_2][K(18\text{-crown-}6)]$ (**1**), as noted by the disappearance of the OH resonances in the ^1H NMR spectrum.

The series of homologous complexes that differ by stepwise protonation provided a unique opportunity to examine the metal's protonation-state dependent electronic environment and catalytic activity. Crystals suitable for X-ray diffraction were obtained for **1**−**4**, and the solid state structures confirm similar primary coordination environments at ruthenium. Fully deprotonated complex **1** adopts C_s symmetry, in which BH_3PI coordinates as a trianionic ligand and a potassium ion is coordinated to both pendent aryloxide bases and capped by an 18-crown-6 unit. Protonation induces the formation of a Ru−O bond in $RuBH_1PI(PPh_3)_2$ (**2**), with the ligand framework enforcing a distorted $\kappa^2(N,O)$ binding mode of one pyridonate arm and a weak hydrogen bond[20] between the OH−O units (O1−O2 = 3.28 Å). The $\kappa^2(N,O)$ coordination is

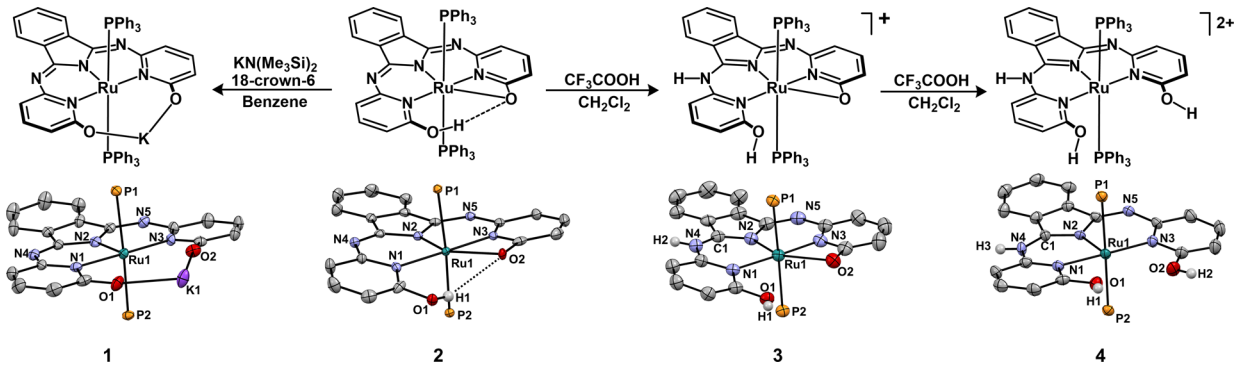

Figure 3. Synthesis of **1**−**4** (above) and solid state structures (below) with thermal ellipsoids depicted at 50% probability (PPh_3 truncated to P, all nonacidic protons omitted, 18-crown-6 omitted in **1**, $CF_3CO_2^-$ anions omitted for clarity).

DOI: 10.1021/jacs.5b08406
J. Am. Chem. Soc. 2015, 137, 12808−12814

preserved upon additional protonation in **3**, which occurs at the imine nitrogen N4. The lengthening of the C1−N4 bond (0.03 Å) and shortening of the C1−N2 bond (0.05 Å) clearly reflects the change in ligand donor properties of the isoindole nitrogen (N2) upon protonation. Further protonation affords a neutral ligand in complex **4**, with no Ru−O bond.

The electronic environment at Ru imparted by each protonation state of the BH_3PI ligand was quantified in **1**−**3**. In addition to the structural metrics, differential pulse voltammetry (DPV) experiments were used to assess electronic differences at the Ru center imposed by each protonation state of BH_3PI in **1**−**3**. The potentials for the first oxidative event undergo an anodic shift with increasing protonation state (E_{Ox} = −660, −460, and 195 mV, vs Fc/Fc^+, for **1**, **2**, and **3** in propylene carbonate/0.1 M [^{n}Bu$_4$][PF$_6$]), which is consistent with a more electron-rich metal center imparted by each successive deprotonation (Figure S67).

E−H Heterolysis: Reactions and Kinetics. We evaluated the cooperative ability of the charge-disparate OH/O$^-$ moieties and ruthenium in **2** to promote heterolytic H−E (E = H or BR_2) bond activation. When treated with H_2 (30 psig) at room temperature, a reaction occurred. The ^{1}H NMR spectrum (−80 °C) revealed a new hydride resonance (δ −10.5) and an acidic proton peak at δ +13.5 that integrated in a 1:2 ratio, consistent with H_2 heterolysis across the metal−ligand framework to form hydride complex **5** in 91% yield. These resonances broadened as the temperature was raised, suggesting a dynamic exchange process. Analysis of the minimum spin−lattice relaxation times, T_1(min), confirmed that the *OH* and hydride peaks undergo chemical exchange and are in close proximity, as noted by their similar short T_1(min) values (76 and 72 ms; −15 °C, 500 MHz). While short T_1 values are often associated with metal η^2-H_2 complexes, they may also reflect unusually short H−H distances in metal hydride complexes engaged in dihydrogen bonds through dipole−dipole relaxation.[21] The unusually short T_1 values in **5** are likely a consequence of close H−H contacts to both of the appended OH groups through bifurcated dihydrogen bonds. Proton/hydride exchange likely proceeds through a transient rotating η^2-H_2 intermediate (Figure 4b), which was not observed.[22] The exchange rate was measured via spin-saturation transfer[23] from −75 to −15 °C, which provided a $\Delta H^{\ddagger}$ and $\Delta S^{\ddagger}$ for the H^+/H^- exchange process of 7.7(2) kcal/mol and −20(1) eu (corresponding to an extrapolated rate of 519 s^{-1} at 25 °C)[24,25] through analysis of an Eyring plot (Figure S69).[23c,25a,26]

The solid state structure of **5** (Figure 4) reveals a Ru−H unit engaged in highly unusual bifurcated dihydrogen bonds with both appended OH groups.[27,28] The Ru−H and both OH protons are clearly distinguishable and located from the difference map. H−H contacts between H1 and H(2,3) of 1.29 and 1.51 Å (average 1.40 Å) reflect strong and extremely short dihydrogen bonds (typical values range from 1.7 to 2.0 Å).[29] Because X-ray diffraction data do not provide precise measurements of H−H distances, we evaluated the M−H···HO distance using through-space dipole−dipole induced nuclear spin relaxation, which afforded an average H−H distance of 1.51 Å at −35 °C.[21] These two measurements, taken through dissimilar methods, showcase the highly coupled proton/hydride environment imposed by the rigid isoindoline ligand and establish the dihydrogen bonds in **5** as among the shortest yet reported.[25a,30]

Following the demonstration of **2** to heterolytically cleave inert H−H bonds, we explored similar reactivity with the B−H bond in pinacolborane (HBPin). When **2** was combined with 2 equiv of HBPin in methylcyclohexane, complex **6** was obtained in 87% yield and was characterized by ^{1}H, ^{31}P, and ^{11}B NMR spectroscopy. The ^{1}H NMR spectrum revealed a hydride signal at δ −11.0 (J_{HB} = 20 Hz), while the ^{31}P and ^{11}B NMR spectra revealed singlets at δ 69.6 and δ 6.0, respectively, consistent with a single phosphorus-containing compound with a tetrahedral boron unit.

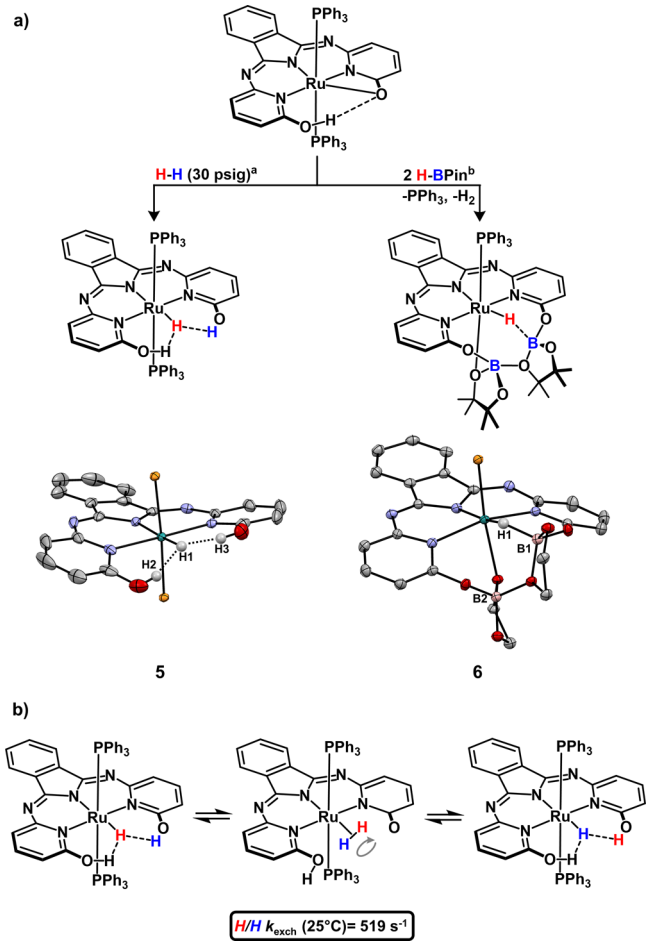

Figure 4. (a) H_2 and HBPin reactivity with **1**. Ellipsoids depicted at 50% probability; PPh_3, truncated to P, H atoms bound to C omitted for clarity; BPin CH_3 omitted. Conditions: (a) C_6H_6, H_2 (30 psig), 25 °C, 4 h. (b) Methylcyclohexane, 25 °C, 1 h. (b) Proposed mechanism for H/H exchange in **5**.

Slow cooling of a solution of **6** in methylcyclohexane afforded crystals suitable for single crystal X-ray diffraction. The solid state structure is analogous to **5**, and similar B−H activation occurs across the Ru−O bond, with the BPin boron (B1) positioned in close proximity to the resulting hydride. The ruthenium hydride (H1) was located from the difference map and freely refined. The B1−H1 contact (1.39 Å) in **6** reflects a weak B−H interaction (cf. B−H in $LiBH_4$ = 1.10 Å)[31] and is similar to a previously reported Ru−H−HBPin coordination complex (1.39 Å).[32] Although bond distances to hydrogen cannot be accurately obtained from typical X-ray data, the low J_{HB} coupling constant (20 Hz; typical B−H single bond coupling is 140 Hz[33]) further supports a weak B−H interaction, indicating that **6** may represent an arrested state of B−H heterolysis. In addition to the HBPin activation across the Ru−O unit, the other appended OH group was transformed into an

DOI: 10.1021/jacs.5b08406
J. Am. Chem. Soc. 2015, 137, 12808−12814

OBPin, with the OBPin unit also participating as a ligand to complete an octahedral geometry about Ru.

Catalytic Hydroboration of Polar Bonds. Based on the rapid H−E activation and exchange rates noted above, we hypothesized that the low kinetic barrier should translate into rapid catalysis. We investigated the catalytic competence of the bifunctional complexes **1**, **2**, and **3** for polar bond hydroboration using ketone and nitrile substrates. When HBPin was introduced to a vial containing 1 equiv of acetophenone and 4 mol % **2** in C_6D_6, 3% conversion to pinacolborato 1-phenylethanol occurred in 20 min at 25 °C. Catalysis was significantly improved for the deprotonated complex, **1**, while fully protonated **3** showed only trace activity. For instance, when identical reaction conditions were used with 100-fold less catalyst loading (0.04 mol % **1**), 54% conversion to borylated 1-phenylethanol occurred (quantitative conversion after 1 h; initial TOF = 1.2(3) s^{-1}).[34] The catalytic activity of **1** is one of the fastest reported for ketone hydroboration at room temperature.[6b,17b,35] For comparison, the unfunctionalized complex $(HRu(bMepi)(PPh_3)_2$, **7**, Figure 5), was significantly slower (initial TOF = 0.037(4) s^{-1}) than **1** under identical conditions. Thus, we found a dramatic effect on catalysis enabled by substituting inert $-CH_3$ groups with polar, reactive $-OH$ groups.

Due to the ability of the bifunctional complexes **1**−**3** to promote rapid ketone hydroboration, we targeted the more challenging hydroboration of nitriles.[11b,17b] Using 5 mol % complex **2** in the presence of 4.5 equiv of HBPin, benzonitrile was converted to the borylated primary amine as the sole product in very low yield (0.05%) after 13 min at 25 °C in C_6D_6 solvent; complex **1** promoted the hydroboration reaction in a much higher yield (66%) after 13 min.[36] Because the electronic environment at ruthenium is regulated by the ligand protonation state, we hypothesized that the strong proton-responsive effect would translate into distinct catalytic rates dependent on protonation state. Initial TOFs for complexes **1**−**3** were determined via *in situ* NMR spectroscopy (Figure 5) and compared with **1**. Complex **3** was inactive for nitrile hydroboration (no product detected). In contrast, catalysis was *turned on* using complex **2** (initial TOF = 2.7(3) × 10^{-4} s^{-1}), and the rate was further accelerated using complex **1** (initial TOF = 1.19(2) × 10^{-2} s^{-1}). We note that single proton transfer events of the appended OH groups promote dramatic changes in reaction rate for **1**−**3**, which serve to both gate and accelerate the nitrile hydroboration reaction.

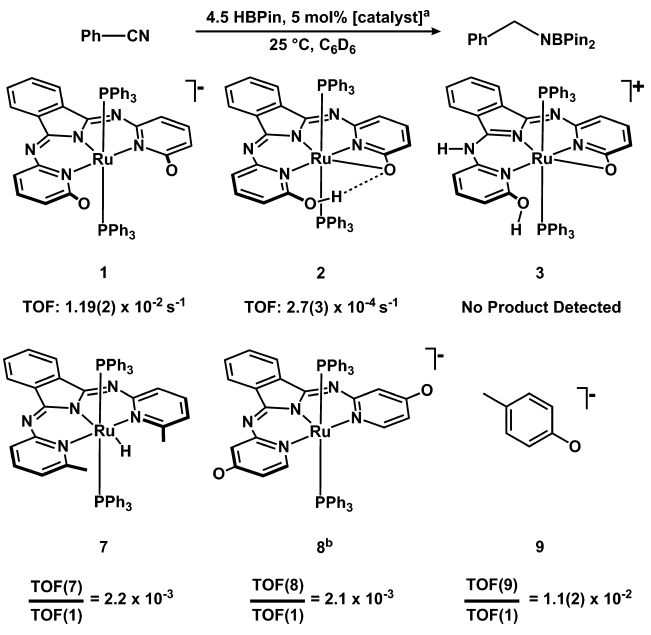

Figure 5. Benzonitrile hydroboration using **1**−**3** and **7**−**9**. K(18-crown-6)$^+$ and $CF_3CO_2^-$ ions omitted for clarity. All anionic species prepared as K(18-crown-6)$^+$ salts. Conditions (a) 0.159 mmol of PhCN, 0.715 mmol of HBPin, 5 μL of $PhSiMe_3$ internal standard, and 5 mol % catalyst in 600 μL of C_6D_6. Initial TOFs determined using ^{1}H NMR spectroscopy. (b) Prepared *in situ* with K(18-crown-6) $N(Me_3Si)_2$.

Catalytic nitrile hydroboration with **1** was general to several *p*-substituted aryl nitriles in moderate to excellent yields (Table 1). The reaction is tolerant to several functional groups, leaving methyl esters (**10m**, 56%), additional nitriles (**10j**, 89%), benzyl ethers (**10c**, 79%), free amines (**10i**, 78%), trifluoromethyl (**10d**, *p*-88%; **10e**, *o*-50%), 2-furyl (**10l**, 96%), and 2-pyridyl (**10k**, 76%) functionality intact. These results suggest that the catalytic hydroboration reaction shows selectivity that is distinct from previously reported heterogeneous and homogeneous reductions; heterogeneous systems cleave benzyl ethers in the presence of nitriles,[16] and homogeneous catalytic systems have not shown selectivity for nitriles over esters.[11b,17b,35a,37]

Mechanistic Analysis. Many reduction reactions involving platinum-group metals have recently been shown to promote the formation of catalytically active nanosized clusters.[38] In order to interrogate the form of the active catalyst (homogeneous or heterogeneous) in the current system, we undertook selective poisoning experiments. The addition of Hg(0) (~800 equiv), which was added after catalysis was

Table 1. Nitrile Hydroboration Scope[a]

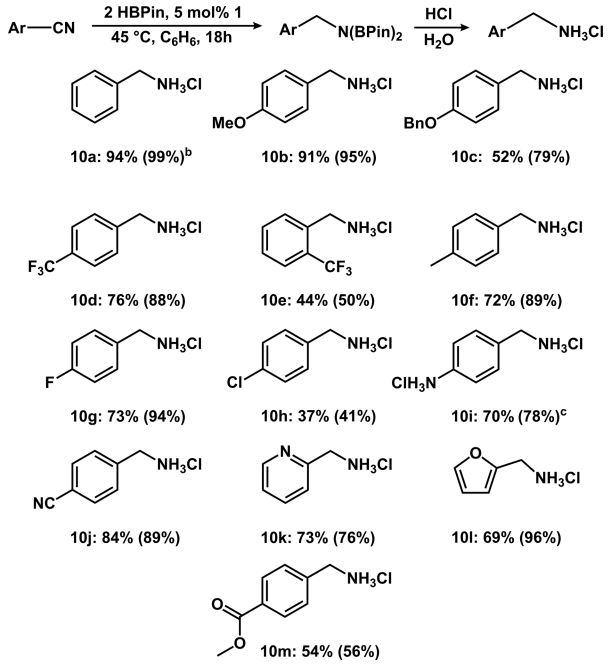

[a]Isolated yields shown; chemical yields of diborylamines in parentheses. Conditions: 0.318 mmol of ArCN, 0.636 mmol of HBPin, 10 μL of $PhSiMe_3$ internal standard, and 5 mol % **1** in 1.2 mL of C_6H_6. Chemical yields determined using ^{1}H NMR spectroscopy. [b]Analogous reaction at 25 °C gives 99% chemical yield. [c]HBPin (4 equiv) added.

DOI: 10.1021/jacs.5b08406
J. Am. Chem. Soc. 2015, 137, 12808−12814

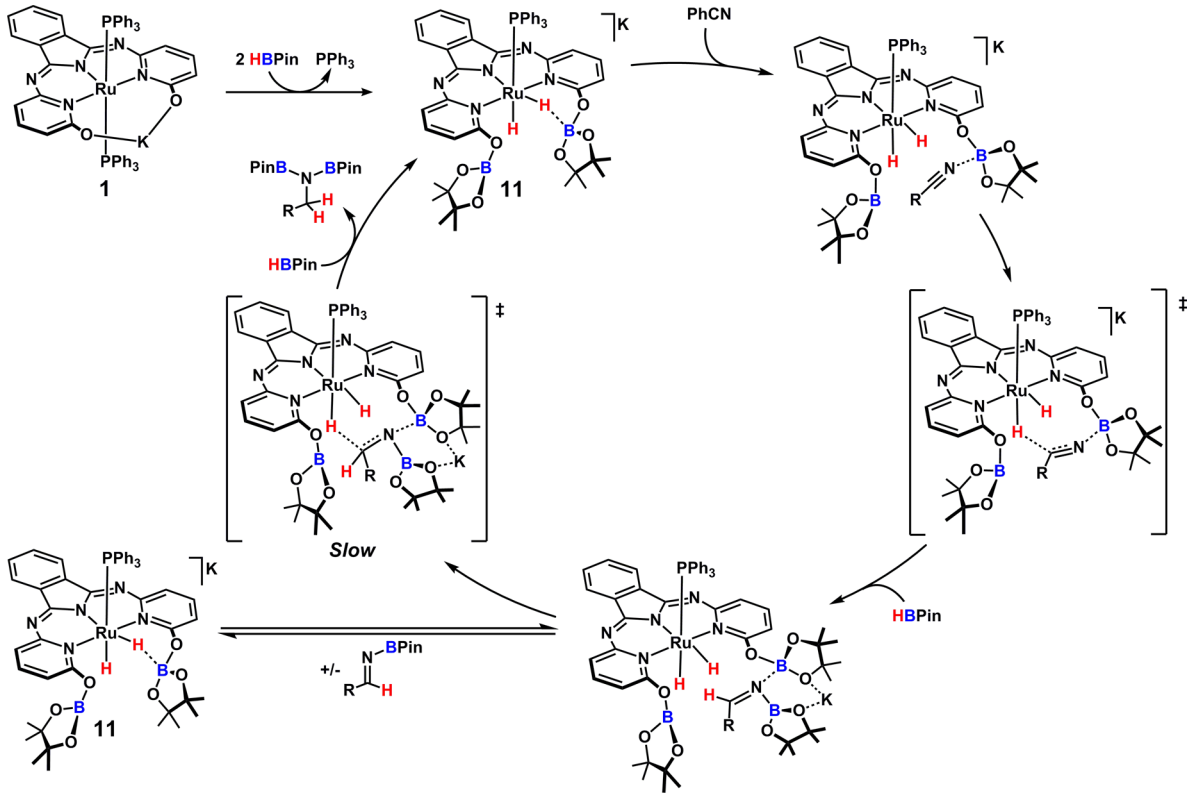

Figure 6. Proposed mechanism for nitrile hydroboration by **1**. 18-Crown-6 omitted for clarity.

initiated, did not appreciably change the overall reaction profile (Figure S84). In addition, we performed substoichiometric ligand poisoning experiments, which are a simple and effective means of assessing whether a given precatalyst forms a catalyst of higher nuclearity. No change in the reaction profile was noted with 0.5 equiv of PMe_3, while complete poisoning required 2 equiv of PMe_3 (Figure S85), inconsistent with a heterogeneous system, where low surface area aggregates are typically poisoned by ≪1 equiv of added ligand poison. Finally, in the absence of any poisoning reagent, highly reproducible (nonsigmoidal) reaction kinetic profiles were observed (Figure S98). The combined results of these tests suggest that the active catalytic species is indeed a homogeneous ruthenium complex.

The protonation-state-dependent rate acceleration for **1**–**3** may be due to regulation of the metal's electronic environment either by changes in the protonation state or alternatively by general base catalysis. To test the efficiency of transition metal-free base catalyzed nitrile hydroboration, we first assessed the pK_a and of the monoprotonated complex, **2** (pK_a(**2**) between 9.5 and 10.8) and selected K(18-crown-6)(*p*-cresolate) (**9**, pK_a = 10.2) as a suitable model base to evaluate general base catalysis.[39] Using identical reaction conditions as described above for nitrile hydroboration, **9** effected the hydroboration reaction with modest efficiency (1.8% conversion in 13 min; initial TOF = 1.4(2) × 10^{-4} s^{-1}), which is 2 orders of magnitude lower than **1**.[40] Activity did not improve in the presence of an equimolar mixture of **7** and **9**, indicating that nitrile activation by coordination to ruthenium is not responsible (or required) for promoting the reduction reaction. The low catalytic activity of a base with a similar pK_b to **1** indicates that the change in the overall protonation state at the metal serves to regulate reactivity at the metal site rather than to promote general base catalysis.[17a,41]

To evaluate the importance of bifunctional E–H activation, we conducted the benzonitrile hydroboration reaction using complex **7**, a variant with inert $-CH_3$ groups rather than $-OH$ groups; this complex had minimal activity (relative TOF to **1** = 2.2 × 10^{-3}). To examine whether catalysis was due to electronic differences imparted by the $-OH$ groups, a variant that moves the $-OH$ groups from the *ortho* to the *para* position (complex **8**) was assessed. Compound **8** presents an electronically similar ligand field yet maintains a distinct spatial orientation of the $-OH$ groups, which is directed *away* from the Ru center. Under identical reaction conditions, **8** was significantly slower than **1** (relative TOF to **1** = 2.1 × 10^{-3}), which suggests that the position of the $-OH$ groups plays a key role to impart hydroboration reactivity. Collectively, the very low catalytic activities of **7**, **8**, and **9** indicate that the identity and position of the $-OH$ groups in **1** is essential for catalytic activity and strongly implicate a crucial role of metal–ligand cooperativity for the B–H heterolysis and transfer steps in nitrile hydroboration.

The above evidence indicates that a cooperative mechanism is operative. At high PhCN (0.2 M) and HBPin (0.5 M) concentrations, present under standard conditions, the reaction is first order in **1** and zero order in both HBPin and benzonitrile (Figure S74–S79),[42] consistent with a mononuclear bifunctional mechanism where H–B activation across the Ru–O unit and ligand substitution/precoordination are *not* rate limiting. Instead, an intramolecular transformation is implicated in the rate-determining step. To distinguish between a limiting outer-sphere or inner-sphere type pathway, we evaluated catalytic reactions *in situ*.

DOI: 10.1021/jacs.5b08406
J. Am. Chem. Soc. 2015, 137, 12808–12814

In order to identify potential catalytic intermediates, stoichiometric reactions between **1** and either HBPin or PhCN were analyzed by NMR spectroscopy. Under conditions of excess PhCN similar to those used in catalysis, 1 equiv of free PPh_3 was observed. Alternatively, in the presence of excess HBPin, conversion to a mixture of hydride containing species was observed in addition to a single phosphorus resonance at δ 39.6. Two of the hydride resonances (δ −5.95 and −10.44) were affected upon selective ^{31}P decoupling, which confirms that both hydrides reside on the same complex as a phosphine ligand. Their $^2J_{HP}$ coupling constants of 103 and 12 Hz are consistent with hydride ligands that are *trans* and *cis* to a phosphine ligand, respectively. We tentatively assign this species as **11**, which we note is coordinatively saturated.

In-situ ^1H NMR spectra revealed that **11** is also present *during* catalysis, and importantly, its concentration tracked with the consumption of nitrile substrate.[43] In addition to observing catalytically relevant intermediates, a species at δ 8.78 was observed and identified as an imine by an $^1H/^{13}C$-gHSQC experiment. During the course of catalysis, the imine peak remained as a singlet (and did not shift its position) and its concentration was 3.5 times greater than the concentration of total ruthenium, consistent with a free, rather than coordinated, imine species. Our proposed mechanism illustrating key species in the nitrile hydroboration reaction is shown in Figure 6 and features BH activation of HBPin by **1**, which can participate in an outer-sphere type transfer of the H and BPin units across the nitrile substrate.[44] We propose that the imine intermediate can dissociate, equilibrating with **11** and that the second hydride transfer is rate limiting. The catalytic hydroboration reaction was hindered in the presence of exogenous alkali metal chelators (18-crown-6 or 2,2,2-cryptand; Figure S83), and the alkali metal is proposed to facilitate the assembly of multiple BPin groups, driving the equilibrium toward coordinated imine. The identification of six-coordinate Ru(II) complexes during catalysis and minimal activity observed for **7** in the presence of **9** suggest that an outer sphere pathway may be more likely than an inner-sphere pathway for rate limiting hydride transfer to the observed imine intermediate. This proposed mechanism is consistent with the observed protonation-state dependent relative rates of **1**−**3**: the increase in metal electron density upon deprotonation leads to a concomitant increase in Ru−H hydricity and the number of hydride ligands, facilitating nucleophilic hydride transfer in the rate-determining step.

CONCLUSIONS

In summary, a proton-responsive bifunctional catalyst for nitrile hydroboration with unprecedented efficiency was developed. Nitrile hydroboration with HBPin has only been reported on one previous occasion with one substrate, and harsh conditions were required.[17a] Compound **1** catalyzes this reaction under mild conditions with a variety of aromatic nitriles. This reaction enables the selective reduction of nitriles to produce synthetically useful diborylamines that can used as organic synthons[45,46] or be easily deprotected.[17b] The designed bifunctional ligand serves a critical role to mediate and regulate this reaction by (1) promoting E−H bond heterolysis, (2) tethering the BPin unit for cooperative substrate interactions, and (3) facilitating proton-switchable regulation of electron density at the metal.

ASSOCIATED CONTENT

Supporting Information

The Supporting Information is available free of charge on the ACS Publications website at DOI: 10.1021/jacs.5b08406.

Synthetic details and characterizations (PDF)

Crystallographic information files for **1**−**6** (CIF)

AUTHOR INFORMATION

Corresponding Author

*nszym@umich.edu

Notes

The authors declare no competing financial interest.

ACKNOWLEDGMENTS

This work was supported by the University of Michigan Department of Chemistry, an NSF-CAREER (Grant CHE-1350877), and the NSF (Grant CHE-0840456) for X-ray instrumentation. N.K.S. is a Dow Corning Assistant Professor and an Alfred P. Sloan Research Fellow. We thank Tim Tseng for providing **8**, Prof. Schindler and Prof. Pecoraro for use of instrumentation, Jeff Kampf for crystallographic assistance, and Cameron Moore and Tim Tseng for productive discussions.

REFERENCES

(1) (a) Zhao, M.; Wang, H.-B.; Ji, L.-N.; Mao, Z.-W. *Chem. Soc. Rev.* **2013**, *42*, 8360. (b) Lancaster, K. In *Molecular Electronic Structures of Transition Metal Complexes I*; Mingos, D. M. P., Day, P., Dahl, J. P., Eds.; Springer: Berlin, Heidelberg, 2012; Vol. *142*, p 119. (c) Natale, D.; Mareque-Rivas, J. C. *Chem. Commun.* **2008**, 425.

(2) (a) Nair, S. K.; Christianson, D. W. *J. Am. Chem. Soc.* **1991**, *113*, 9455. (b) Machczynski, M. C.; Gray, H. B.; Richards, J. H. *J. Inorg. Biochem.* **2002**, *88*, 375.

(3) (a) Ringenberg, M. R.; Rauchfuss, T. B. *Eur. J. Inorg. Chem.* **2012**, *2012*, 490. (b) Ghosh, S.; Dey, A.; Sun, Y.; Scholes, C. P.; Solomon, E. I. *J. Am. Chem. Soc.* **2009**, *131*, 277. (c) Dixon, N. A.; McQuarters, A. B.; Kraus, J. S.; Soffer, J. B.; Lehnert, N.; Schweitzer-Stenner, R.; Papish, E. T. *Chem. Commun.* **2013**, *49*, 5571. (d) Lin, I.-J.; Gebel, E. B.; Machonkin, T. E.; Westler, W. M.; Markley, J. L. *Proc. Natl. Acad. Sci. U. S. A.* **2005**, *102*, 14581. (e) Fujita, K.-i.; Tanino, N.; Yamaguchi, R. *Org. Lett.* **2007**, *9*, 109.

(4) (a) Hull, J. F.; Himeda, Y.; Wang, W.-H.; Hashiguchi, B.; Periana, R.; Szalda, D. J.; Muckerman, J. T.; Fujita, E. *Nat. Chem.* **2012**, *4*, 383. (b) Nieto, I.; Livings, M. S.; Sacci, J. B.; Reuther, L. E.; Zeller, M.; Papish, E. T. *Organometallics* **2011**, *30*, 6339. (c) Hashiguchi, B. G.; Young, K. J. H.; Yousufuddin, M.; Goddard, W. A.; Periana, R. A. *J. Am. Chem. Soc.* **2010**, *132*, 12542.

(5) (a) Eisenstein, O.; Crabtree, R. H. *New J. Chem.* **2013**, *37*, 21. (b) Noyori, R.; Ohkuma, T. *Angew. Chem., Int. Ed.* **2001**, *40*, 40. (c) Clapham, S. E.; Hadzovic, A.; Morris, R. H. *Coord. Chem. Rev.* **2004**, *248*, 2201.

(6) (a) Watanabe, M.; Murata, K.; Ikariya, T. *J. Am. Chem. Soc.* **2003**, *125*, 7508. (b) Koren-Selfridge, L.; Londino, H. N.; Vellucci, J. K.; Simmons, B. J.; Casey, C. P.; Clark, T. B. *Organometallics* **2009**, *28*, 2085. (c) Anaby, A.; Butschke, B.; Ben-David, Y.; Shimon, L. J. W.; Leitus, G.; Feller, M.; Milstein, D. *Organometallics* **2014**, *33*, 3716. (d) Bolaño, T.; Esteruelas, M. A.; Gay, M. P.; Oñate, E.; Pastor, I. M.; Yus, M. *Organometallics* **2015**, *34*, 3902.

(7) (a) Wang, W.-H.; Muckerman, J. T.; Fujita, E.; Himeda, Y. *New J. Chem.* **2013**, *37*, 1860. (b) Moore, C. M.; Dahl, E. W.; Szymczak, N. K. *Curr. Opin. Chem. Biol.* **2015**, *25*, 9.

(8) The only example of a transition metal hydrofunctionalization catalyst with three isolable protonation states did not include a comparison of catalytic activity among all three protonation states. See: Toda, T.; Kuwata, S.; Ikariya, T. *Chem. - Eur. J.* **2014**, *20*, 9539.

DOI: 10.1021/jacs.5b08406
J. Am. Chem. Soc. 2015, 137, 12808−12814

(9) (a) Himeda, Y.; Onozawa-Komatsuzaki, N.; Sugihara, H.; Kasuga, K. *J. Photochem. Photobiol., A* **2006**, *182*, 306. (b) Terrade, F. G.; Lutz, M.; van der Vlugt, J. I.; Reek, J. N. H. *Eur. J. Inorg. Chem.* **2014**, *2014*, 1826.
(10) (a) Moore, C. M.; Szymczak, N. K. *Chem. Commun.* **2013**, *49*, 400. (b) Tutusaus, O.; Ni, C.; Szymczak, N. K. *J. Am. Chem. Soc.* **2013**, *135*, 3403. (c) Moore, C. M.; Szymczak, N. K. *Dalton Transactions* **2012**, *41*, 7886. (d) Moore, C. M.; Quist, D. A.; Kampf, J. W.; Szymczak, N. K. *Inorg. Chem.* **2014**, *53*, 3278.
(11) (a) Stahl, T.; Müther, K.; Ohki, Y.; Tatsumi, K.; Oestreich, M. *J. Am. Chem. Soc.* **2013**, *135*, 10978. (b) Lu, Z.; Williams, T. J. *Chem. Commun.* **2014**, *50*, 5391.
(12) For recent examples of catalytic noncooperative polar bond hydroborations, see: (a) Arrowsmith, M.; Hadlington, T. J.; Hill, M. S.; Kociok-Köhn, G. *Chem. Commun.* **2012**, *48*, 4567. (b) Hadlington, T. J.; Hermann, M.; Frenking, G.; Jones, C. *J. Am. Chem. Soc.* **2014**, *136*, 3028. (c) Chong, C. C.; Kinjo, R. *ACS Catal.* **2015**, *5*, 3238.
(13) Westcott, S. A.; Baker, R. T. In *Modern Reduction Methods*; Andersson, P. G., Munslow, I. J., Eds.; Wiley-VCH Verlag GmbH & Co. KGaA: Weinheim, Germany, 2008; p 297.
(14) (a) Chae, M. J.; Song, J.-I.; An, D.-K. *Bull. Korean Chem. Soc.* **2007**, *28*, 2517. (b) Haddenham, D.; Pasumansky, L.; DeSoto, J.; Eagon, S.; Singaram, B. *J. Org. Chem.* **2009**, *74*, 1964.
(15) Although $NaBH_4$ in carboxylic acid media provides some selectivity for nitriles, the acidic conditions are not compatible with many substrates. See: Gribble, G. W. *Chem. Soc. Rev.* **1998**, *27*, 395.
(16) Jeon, Y. T.; Yang, W.; Qiao, J. X.; Li, L.; Ruel, R.; Thibeault, C.; Hiebert, S.; Wang, T. C.; Wang, Y.; Liu, Y.; Clark, C. G.; Wong, H. S.; Zhu, J.; Wu, D.-R.; Sun, D.; Chen, B.-C.; Mathur, A.; Chacko, S. A.; Malley, M.; Chen, X.-Q.; Shen, H.; Huang, C. S.; Schumacher, W. A.; Bostwick, J. S.; Stewart, A. B.; Price, L. A.; Hua, J.; Li, D.; Levesque, P. C.; Seiffert, D. A.; Rehfuss, R.; Wexler, R. R.; Lam, P. Y. S. *Bioorg. Med. Chem. Lett.* **2014**, *24*, 1294.
(17) (a) Eisenberger, P.; Bailey, A. M.; Crudden, C. M. *J. Am. Chem. Soc.* **2012**, *134*, 17384. (b) Khalimon, A. Y.; Farha, P.; Kuzmina, L. G.; Nikonov, G. I. *Chem. Commun.* **2012**, *48*, 455.
(18) (a) Tseng, K.-N. T.; Kampf, J. W.; Szymczak, N. K. *Organometallics* **2013**, *32*, 2046. (b) Tseng, K.-N. T.; Rizzi, A. M.; Szymczak, N. K. *J. Am. Chem. Soc.* **2013**, *135*, 16352. (c) Tseng, K.-N. T.; Kampf, J. W.; Szymczak, N. K. *ACS Catal.* **2015**, *5*, 5468.
(19) Takaoka, A.; Mendiratta, A.; Peters, J. C. *Organometallics* **2009**, *28*, 3744.
(20) Steiner, T. *Angew. Chem., Int. Ed.* **2002**, *41*, 48.
(21) Desrosiers, P. J.; Cai, L.; Lin, Z.; Richards, R.; Halpern, J. *J. Am. Chem. Soc.* **1991**, *113*, 4173.
(22) The 1:2 integration of the hydride to OH protons, as well as the absence of any other low-T_1 resonances, is not consistent with a Ru–(H_2) intermediate under these conditions.
(23) (a) Jarek, R. L.; Flesher, R. J.; Shin, S. K. *J. Chem. Educ.* **1997**, *74*, 978. (b) Henry, R. M.; Shoemaker, R. K.; DuBois, D. L.; DuBois, M. R. *J. Am. Chem. Soc.* **2006**, *128*, 3002. (c) Hulley, E. B.; Helm, M. L.; Bullock, R. M. *Chem. Sci.* **2014**, *5*, 4729.
(24) In many recent reports (see ref 25), low temperature exchange rates have been scaled to 293 K through speculative estimates of activation entropy, which may lead to inflated extrapolated rates. Adopting similar treatment, our rate at 293 K is 1.9×10^5 s^{-1} rather than 520 s^{-1}. The large negative entropy value in **5** may reflect of a loss of electronic entropy and symmetry in the transition state for hydride protonation.
(25) (a) Liu, T.; Wang, X.; Hoffmann, C.; DuBois, D. L.; Bullock, R. M. *Angew. Chem., Int. Ed.* **2014**, *53*, 5300. (b) Hulley, E. B.; Welch, K. D.; Appel, A. M.; DuBois, D. L.; Bullock, R. M. *J. Am. Chem. Soc.* **2013**, *135*, 11736.
(26) Curtis, C. J.; Miedaner, A.; Ciancanelli, R.; Ellis, W. W.; Noll, B. C.; Rakowski DuBois, M.; DuBois, D. L. *Inorg. Chem.* **2003**, *42*, 216.
(27) There is one previously reported bifurcated intramolecular hydrogen bond in a metal complex, with a long H–H contact of 1.8 Å. Park, S.; Ramachandran, R.; Lough, A. J.; Morris, R. H. *J. Chem. Soc., Chem. Commun.* **1994**, 2201.
(28) (a) Lee, D.-H.; Patel, B. P.; Crabtree, R. H.; Clot, E.; Eisenstein, O. *Chem. Commun.* **1999**, 297. (b) Wessel, J.; Lee, J. C.; Peris, E.; Yap, G. P. A.; Fortin, J. B.; Ricci, J. S.; Sini, G.; Albinati, A.; Koetzle, T. F.; Eisenstein, O.; Rheingold, A. L.; Crabtree, R. H. *Angew. Chem., Int. Ed. Engl.* **1995**, *34*, 2507.
(29) Custelcean, R.; Jackson, J. E. *Chem. Rev.* **2001**, *101*, 1963.
(30) (a) Carroll, M. E.; Barton, B. E.; Rauchfuss, T. B.; Carroll, P. J. *J. Am. Chem. Soc.* **2012**, *134*, 18843. (b) Huynh, M. T.; Wang, W.; Rauchfuss, T. B.; Hammes-Schiffer, S. *Inorg. Chem.* **2014**, *53*, 10301.
(31) Filinchuk, Y.; Chernyshov, D.; Cerny, R. *J. Phys. Chem. C* **2008**, *112*, 10579.
(32) Gunanathan, C.; Hölscher, M.; Pan, F.; Leitner, W. *J. Am. Chem. Soc.* **2012**, *134*, 14349.
(33) Nöth, H.; Wrackmeyer, B. In *Nuclear Magnetic Resonance Spectroscopy of Boron Compounds*; Nöth, H., Wrackmeyer, B., Eds.; Springer: Berlin, Heidelberg, 1978; Vol. *14*, p 109.
(34) Initial turnover frequency was calculated by determining the initial reaction rate through line fitting of product concentration during the first 10% of reaction progress, then dividing the reaction rate by the catalyst concentration. For a discussion of the merits of using initial TOF, see: Kozuch, S.; Martin, J. M. L. *ACS Catal.* **2012**, *2*, 2787.
(35) (a) Arrowsmith, M.; Hadlington, T. J.; Hill, M. S.; Kociok-Köhn, G. *Chem. Commun.* **2012**, *48*, 4567. (b) Hadlington, T. J.; Hermann, M.; Frenking, G.; Jones, C. *J. Am. Chem. Soc.* **2014**, *136*, 3028. (c) Oluyadi, A. A.; Ma, S.; Muhoro, C. N. *Organometallics* **2013**, *32*, 70.
(36) Under the same reaction conditions (25 °C, C_6D_6), H_2 (100 psi) or $NaBH_4$ did not react with benzonitrile to form benzylamine.
(37) (a) Arrowsmith, M.; Hill, M. S.; Hadlington, T.; Kociok-Köhn, G.; Weetman, C. *Organometallics* **2011**, *30*, 5556. (b) Mukherjee, D.; Ellern, A.; Sadow, A. D. *Chemical Science* **2014**, *5*, 959.
(38) (a) Widegren, J. A.; Finke, R. G. *J. Mol. Catal. A: Chem.* **2003**, *198*, 317. (b) Crabtree, R. H. *Chem. Rev.* **2012**, *112*, 1536.
(39) Due to the pK_a difference between **1** and **2**, the same concentration of catalyst was used to compare the catalytic activity of **1** and **7**. See Supporting Information for experimental details.
(40) See Supporting Information for kinetic experimental details.
(41) Query, I. P.; Squier, P. A.; Larson, E. M.; Isley, N. A.; Clark, T. B. *J. Org. Chem.* **2011**, *76*, 6452.
(42) We note that these orders are defined at the high substrate concentrations used during the initial portion of catalysis. At low concentrations (<0.5 and <0.2 M for HBPin and PhCN, respectively), there is a positive correlation between concentration and the initial rate.
(43) Compound **11** is proposed to engage in an equilibrium reaction prior to the turnover limiting step. Other reactions in the catalytic cycle likely also participate in equilibrium reactions with substrates, consistent with the observed saturation kinetics in HBPin and PhCN at high concentrations.
(44) While an inner sphere pathway is also possible, the high concentration of coordinatively saturated **11** in solution, in addition to the minimal activity observed for **7** in the presence of **9**, suggest an outer sphere pathway may be more likely.
(45) Compounds containing heteroatom–boron bonds have gained recent interest as organic synthons. See: Hirner, J. J.; Faizi, D. J.; Blum, S. A. *J. Am. Chem. Soc.* **2014**, *136*, 4740. Chong, E.; Blum, S. A. *J. Am. Chem. Soc.* **2015**, *137*, 10144.
(46) The diborylamine products react with benzaldehyde to form imines in the absence of a desiccant via the generation of $BPin_2O$; see Supporting Information for details. For examples with $PhCH_2N(BCat)_2$, see ref 17b.

DOI: 10.1021/jacs.5b08406
J. Am. Chem. Soc. 2015, 137, 12808–12814